A Detailed Testing Procedure of Numerical Differential Protection Relay for EHV Auto Transformer

Umer Ehsan [1,2], Muhammad Jawad [1,*], Umar Javed [1,3], Khurram Shabih Zaidi [1], Ateeq Ur Rehman [4], Anton Rassõlkin [5], Maha M. Althobaiti [6], Habib Hamam [7,8,9] and Muhammad Shafiq [10,*]

[1] Department of Electrical and Computer Engineering, Lahore Campus, COMSATS University Islamabad, Islamabad 54000, Pakistan; umer.ehsan@yahoo.com (U.E.); umarjaved636@gmail.com (U.J.); kzaidi@cuilahore.edu.pk (K.S.Z.)
[2] National Transmission and Despatch Company Limited, Lahore 54000, Pakistan
[3] Riphah College of Science and Technology, Lahore Campus, Riphah International University, Islamabad 54000, Pakistan
[4] Department of Electrical Engineering, Government College University, Lahore 54000, Pakistan; ateqrehman@gmail.com
[5] Department of Electrical Power Engineering & Mechatronics, Tallinn University of Technology, 12616 Tallinn, Estonia; anton.rassolkin@taltech.ee
[6] Department of Computer Science, College of Computing and Information technology, Taif University, P.O. Box 11099, Taif 21944, Saudi Arabia; Maha_m@tu.edu.sa
[7] Faculty of Engineering, Uni de Moncton, Moncton, NB E1A 3E9, Canada; habib.hamam@umoncton.ca
[8] Spectrum of Knowledge Production & Skills Development, Sfax 3027, Tunisia
[9] Department of Electrical and Electronic Engineering Science, School of Electrical Engineering, University of Johannesburg, Johannesburg 2006, South Africa
[10] Department of Information and Communication Engineering, Yeungnam University, Gyeongsan 38541, Korea
[*] Correspondence: mjawad@cuilahore.edu.pk (M.J.); shafiq@ynu.ac.kr (M.S.)

Abstract: In power systems, the programmable numerical differential relays are widely used for the protection of generators, bus bars, transformers, shunt reactors, and transmission lines. Retrofitting of relays is the need of the hour because lack of proper testing techniques and misunderstanding of vital procedures may result in under performance of the overall protection system. Lack of relay's proper testing provokes an unpredictability in its behavior, that may prompt tripping of a healthy power system. Therefore, the main contribution of the paper is to prepare a step-by-step comprehensive procedural guideline for practical implementation of relay testing procedures and a detailed insight analysis of relay's settings for the protection of an Extra High Voltage (EHV) auto transformer. The experimental results are scrutinized to document a detailed theoretical and technical analysis. Moreover, the paper also covers shortcomings of existing literature by documenting specialized literature that covers all aspects of protection relays, i.e., from basics of electromechanical domain to the technicalities of the numerical differential relay covering its detailed testing from different reputed manufacturers. A secondary injection relay test set is used for detailed testing of differential relay under test, and the S1 Agile software is used for protection relay settings, configuration modification, and detailed analysis.

Keywords: current transformers; current measurement; power system protection; power transformers; relays; testing

1. Introduction

In modern Extra High Voltage (EHV) power networks, the protection of the power system is continuously being upgraded by the replacement of old electromechanical protection relays with the new microprocessor based numerical protection relays known as Intelligent Electronic Devices (IEDs). Retrofitting of numerical protection relays is essential and currently an ongoing process throughout power transmission networks. If it is not

properly configured and tested or the settings are inappropriate due to lack of its technical knowledge, then the relay can exhibit unpredictable behavior [1]. Due to the fact, the relay may not sense faulty conditions at all or may cause tripping in a healthy condition. Such behavior of numerical protection relay is highly undesirable and ultimately results in frequent outages in power systems along with massive revenue loss. To mitigate such undesired situations and system disturbances, it is necessary to conduct their detailed testing.

The power system under test is a three-phase solidly grounded, with a maximum nominal phase-to-phase voltage level equal to 500 kV. The generation voltage is less than or equal to 23 kV and is stepped up to the desired transmission voltage level through station transformers. The transmission voltage is either 500 or 220 kV. To step down voltage level from 500 to 220 kV and from 220 to 132 kV, auto transformers are employed. Moreover, the 132 kV voltage level is stepped down to 11.5 kV through conventional power transformer. The SLD of the system showing all voltage levels is depicted in Figure 1 [2]. In an existing power system of Pakistan, two differential relays named as main differential relay and rough balance differential relay are installed for protection of 500 kV/220 kV auto transformer and 220 kV/132 kV auto transformer, respectively [3]. Through continuous monitoring of the protection relays, it is ensured that any undesired situation or fault is dealt with using proper response and the faulty portion is isolated from the healthy system with high speed, accuracy, selectivity, and reliability.
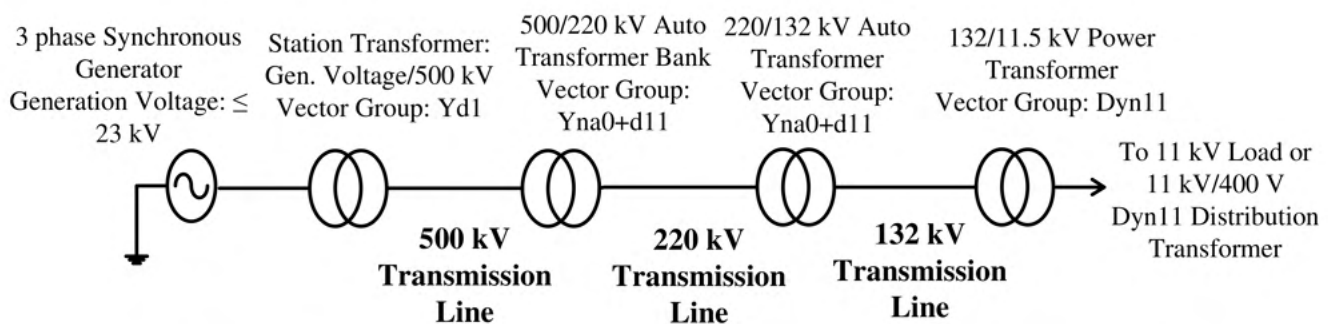

Figure 1. Single line diagram showing all voltage levels of the power system in Pakistan [2].

In the literature, very few research articles are published that discuss theoretical details of IEDs and different testing techniques. In [4], theoretical aspects in testing of the microprocessor based numerical protection relays are discussed. The author discusses the concepts, such as vector group of transformers, interposing CTs, and zero sequence filtering in detail. Moreover, the authors also describe the concepts for pickup test and bias characteristics test. However, the paper lacks a double phase pickup test and harmonic restraint testing of numerical differential relay that are of vital importance. In [5], a study of differential relay is presented considering power system disturbances and the behavior of the numerical differential relay is analyzed in detail; however, its exact threshold settings and set points are not verified. A novel technique for determining the settings of numerical differential relay is proposed in [6]. The authors have used a software-based simulator that utilizes iterations for the determination of settings. Furthermore, enhancement techniques for power transformer differential protection are described in [7], in which the author also discussed internal and external fault cases for differential protection and conducted a simulation testing through real-time digital simulation.

The actuation of transformer differential protection is conditional to the presence of existing internal transformer faults that may deteriorate a transformer's health. Several methods have been developed to perform condition monitoring of a transformer's health [8]. One such method is Frequency Response Analysis (FRA), which deals with analyzing the frequency response of a transformer on application of signal with frequency ranging from several hundred to several mega Hertz (low, mid, and high frequency bands) and compares it with the pre-commissioning or factory testing signal of transformers. In [8],

the authors provide comprehensive guidelines for interpretation and evaluation of FRA of transformers. Moreover, in [9], the authors discuss valuable insight on understanding FRA signatures and the effect of several transformer faults on FRA signature. The faults include axial displacement, bushing fault, radial deformation, loss of clamping pressure, inter-disk fault, and short circuit fault.

To the best of the author's knowledge, there is no formal guideline and detailed study available to the research community and power system protection experts that thoroughly discusses the testing procedures for numerical differential relays as a single document. Therefore, to fill this literature gap, the main purpose of this research work is to prepare and compose a step-by-step detailed manual that can provide a complete guideline for the practical implementation of relay testing procedures and thorough numerical analysis that one can follow to check the health and functionality of a differential protection relay installed at EHV auto transformer. A real-time result analysis is performed on the differential relay installed for protection of 160 MVA, 220/132 kV Auto Transformer located at 220 kV Grid Station NTDC Kala Shah Kaku, Lahore, Pakistan. The experimental results are scrutinized to document a detailed theoretical and technical analysis. In light of the above stated actualities, the main contributions of the paper are:

- Detailed insight analysis of numerical differential relay settings including connection details, operating principle, and biasing characteristics. Moreover, important transformer considerations are also discussed.
- A detailed testing procedure of numerical differential relay is conducted through secondary injection testing with actual settings. The testing results include measurement test, pickup test, trip-time test, stability test, bias characteristics test, 2nd and 5th harmonic restraints test, and high stage 1 and high stage 2 test.
- A detailed theoretical and technical analysis is conducted and documented to analyze the practical results.

The remaining paper is organized as follows: Section 2 discusses differential relay architecture and differential relay considerations for transformer application briefly. Section 3 focuses towards Matching Current Transformers or Interposing Current Transformers. The key settings implemented in the relay under test are described in Section 4. Section 5 discusses the testing of differential relay in detail. Section 6 focuses on a result discussion of the tests performed. The paper is concluded in Section 7 along with future suggestions.

2. Differential Relay

Figure 2a shows the single line diagram for connections of differential relay based on Kirchhoff's current law [10]. In Figure 2a, the current transformers are used as current sensors that essentially stepdown current with high fidelity [11]. The relay receives input from CTs, and continuously monitors and compares current. If any mismatch is observed beyond the defined setting, then the trip command is initiated, which isolates the protected object from the power system. Differential relay compares the magnitude and phase angle of the currents available at its terminals and remains stable if the vector sum of compared currents is less than the threshold setting in its internal differential coils [5]. Figure 2b explains the single-phase schematic drawing for basic operating principle of the differential relay. The comparison or vector sum is performed in the differential coil C of the relay and resultant current is called differential current I_{diff}. The I_{diff} is zero if vector sum of currents from side A (I_A) and side B (I_B) is zero. The minimum value of the differential current I_{diff} at which the relay operates is controlled by a setting called I_{diff} pickup. A minute spill current normally flows through the relay due to the CT errors and losses [12].

In Figure 2b, the restraining coils A and B are also called biasing coils. As the current through protected equipment increases, for example in case of through fault, spill current increases proportionally. The relay may operate during through fault due to spill current since the I_{diff} pickup was the only setting of the differential relay, which is highly undesirable. To mitigate this issue, restraining or biasing is provided based on the loading condition of the protected object through restraining coils, and their setting results in

percentage bias characteristics (slope characteristics) of the relay, which essentially results in restraining the operation of the relay [13]. The restraint (biasing) characteristics provide stability to the differential relay during normal and through fault scenarios; therefore, the differential relays are called percentage biased differential relays.
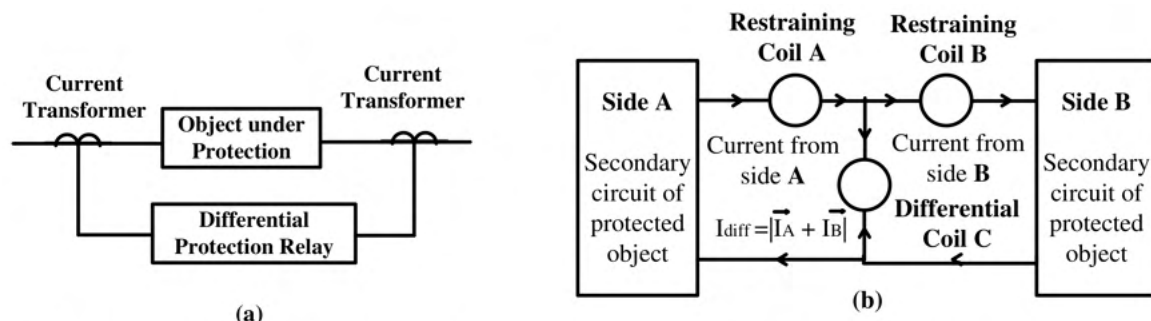

Figure 2. Differential protection relay: (**a**) single line diagram with connections [10] and (**b**) basic operating principle [13].

3. Transformers

A transformer is a static electric machine and works on electromagnetic induction principles. It is used to transfer power from one voltage level to another one while maintaining electrical isolation between different voltage levels and can be controlled by varying the number of turns of each winding. However, the voltage per turn ratio remains constant across its windings. The nominal current of each winding can be calculated by using Equation (1) [4].

$$I_{nom} = \frac{Power\ Rating_{KVA}}{\sqrt{3} \times Ph - Ph\ Voltage\ rating_{KV}} \tag{1}$$

The transformers occupy less geographical area that makes them well suited to be protected through differential protection. The differential protection has a very crisp and well-defined zone of protection. The zone of protection is between the CTs that are feeding the differential relay. Some important considerations regarding transformers must be considered before further delving into application of differential relay for the protection of transformers. In a nutshell, the transformer differential relay must cater for the following characteristics of a transformer.

- Differential relay should cater Vector Group of Transformer [14,15], Zero Sequence Current Flows [16], On Load Tap Changers [17], and must not initiate tripping during normal operation of transformer including energization of transformer (Inrush Current [18,19]), over fluxing [20], and tap changer operation.
- Differential relay should remain stable during through fault even if the CT saturation of one or more CTs occur [21,22].
- Differential relay should only initiate tripping during in-zone fault (fault inside protection zone of differential relay [23]).

4. Matching Current Transformers of Interposing Transformers

When no fault occurs in the differential protection zone during normal operation of a transformer, the current in differential coils of the differential relay should be equal in magnitude but with 180-degree phase shift. However, secondary currents from CTs mostly differ in magnitude and phase angle; therefore, the secondary currents cannot be directly applied to the differential coils of the relay and are conditioned and modified before applying to them so that the relay remains stable (ideally $I_{diff} = 0$) during the transformer's normal operation. The conditioning and matching of CT secondary currents are performed through Matching Current Transformers (MCT) or Interposing CT [4]. The matching CTs also performs zero-sequence filtering whenever required in the secondary circuit.

Figure 3a shows the connection diagram of the differential relay with two windings of the transformer. The transformer under consideration is 220/132/11 kV, 160/160/30 MVA auto transformer with vector group Yna0 + d11. High voltage side (primary winding) terminals are marked as A, B, and C while the secondary winding terminals (132 kV side) are marked as Am, Bm, and Cm. The neutral terminal is grounded and marked as O. Tertiary winding terminals (11 kV side) are marked as a, b, x, and c. Tertiary delta is unloaded, kept close through external jumper between terminal x and terminal c and is not wired to the differential relay. The external jumper between terminals x and c is connected to ground.

The secondary side of both main CTs is star connected and the star point is towards the auto transformer and is grounded at one point only. The secondary CT circuit from 220 and 132 kV side terminates into the current elements of the differential relay as shown in Figure 3a. The dotted box marked as "D" inside differential relay contains MCTs, restraining coils, differential coils, and harmonic restraining coils. In modern differential relays, all such coils are implemented through an algorithm. Matching CT's configuration and vector group depends on transformer under protection and may vary from manufacturer to manufacturer as per their protection design. Figure 3b shows the inside architecture of the dotted box D from Figure 3a [24]. The red (R), yellow (Y), blue (B), and neutral (N) currents from HV CT secondary side is shown as $I_{HV\ sec-R}$, $I_{HV\ sec-Y}$, $I_{HV\ sec-B}$, and $I_{HV\ sec-N}$, respectively. Similarly, for the LV CT secondary side they are shown as $I_{LV\ sec-R}$, $I_{LV\ sec-Y}$, $I_{LV\ sec-B}$, and $I_{LV\ sec-N}$, respectively. Both HV and LV side MCT is in star–delta–star configuration. The delta winding traps the zero-sequence current. In this particular case, both HV and LV MCT are used for magnitude compensation and phase introduced by them will be 0. MCT configurations for relay type P642 under different vector groups of transformers are as follows.
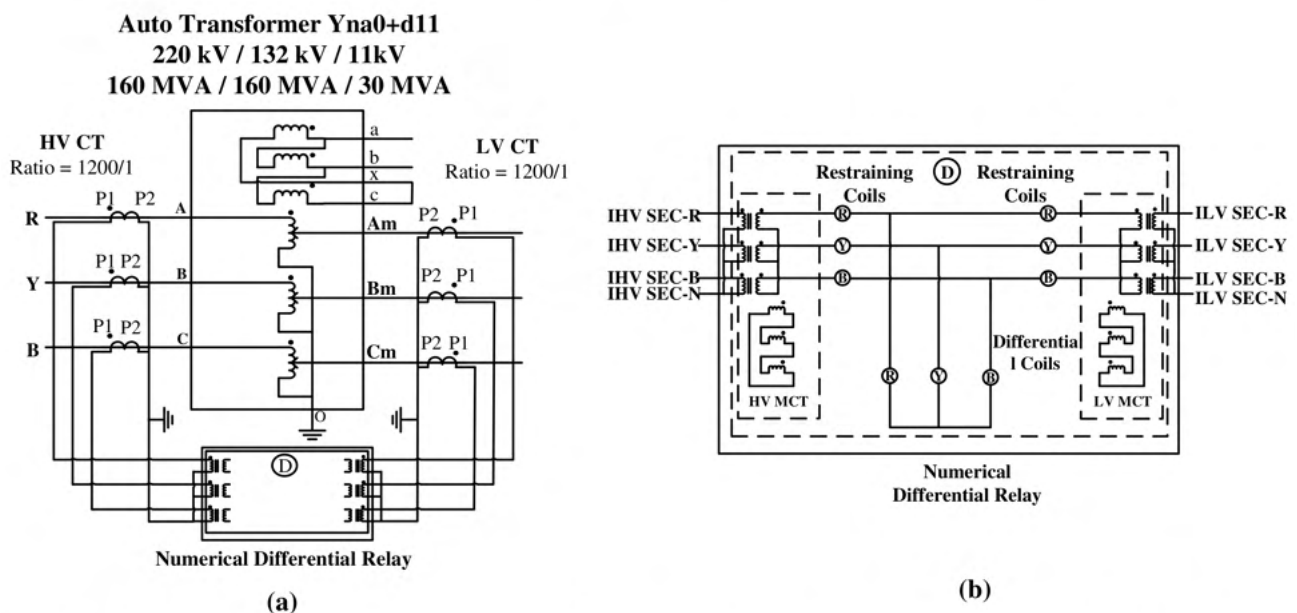
Figure 3. Differential relay circuit [24]: (**a**) connection diagram with two windings of transformer, and (**b**) matching CTs, restraining coils, and differential coils implemented in differential relay through algorithm.

4.1. HV MCT

Transformer HV side matching CTs, irrespective of transformer's vector group under protection are of either star–delta–star or star–star configuration. Star–delta–star configuration is used for magnitude compensation and zero sequence filtering whereas star–star configuration performs magnitude compensation only.

4.2. LV MCT

If the main transformer has a vector group of YyX or DdX (where X is any even integer from 0 to 11 indicating phase shift between HV and LV windings), then LV MCT will be star–star Z (when zero sequence current filtering is disabled) or star–delta–star Z (when zero sequence current filtering is enabled). The Z is the phase shift introduced by LV MCT for the compensation of phase shift introduced by the vector group of the main transformer. The delta is only introduced when zero sequence current filtering is required. Similarly, if the main transformer has vector group of YdX or DyX (where X is any odd integer from 1 to 11 showing phase shift between primary and secondary winding), then LV MCT will be star–delta Z. LV MCT provides necessary phase compensation in addition to the magnitude compensation and zero-sequence filtering (if required). Table 1 shows different vector groups of transformer and corresponding LV MCT configuration with required phase shift when the vector group of transformers under protection is YyX, DdX, YdX, or DyX.

Table 1. LV MCT vector group configuration for transformers: (**A**) with vector group YyX or DdX, (**B**) transformers with vector group YdX or DyX.

Sr. No.	(A) VG YyX or DdX		(B) VG YdX or DyX	
	Transformer Vector Group	LV MCT Vector Group	Transformer Vector Group	HV MCT Vector Group
1	Yy0 or Dd0	Yy0	Yd1 or Dy1	Yd11
2	Yy2 or Dd2	Yy10	Yd3 or Dy3	Yd9
3	Yy4 or Dd4	Yy8	Yd5 or Dy5	Yd7
4	Yy6 or Dd6	Yy6	Yd7 or Dy7	Yd5
5	Yy8 or Dd8	Yy4	Yd9 or Dy9	Yd3
6	Yy10 or Dd10	Yy2	Yd11 or Dy11	Yd1

5. Settings Implemented in Differential Relay

The S1 Agile software is used for implementation of settings in differential relay P642 (Make: Alstom [24]) [25]. The CT ratio data, transformer data, and differential relay settings implemented in the differential relay are shown in Tables 2–4, respectively. In Table 4, the setting 'T1 CT' with address '0A.10' corresponds to HV side CT and setting of HV CT ratio is 1200:1. The setting 'Polarity' is set to 'standard' that shows the star point of HV CT is towards transformer. Moreover, the setting 'T2 CT' with address '0A.14' corresponds to LV side CT and setting of LV CT Ratio is also 1200:1. The setting 'Polarity' is set to 'standard' that shows the star point of the LV CT is towards the transformer.

Table 2. CT data implementation in differential relay on 220 kV GS KSK 160 MVA transformer T2.000.

CT and VT Ratios	Value	Address (C.R)
Aux' VT Location	HV	0A.02
Aux' VT Primary	220.0 kV	0A.07
Aux' VT Sec' y	110.0 V	0A.08
T1 CT		0A.10
Polarity	Standard	0A.11
Primary	1200 A	0A.12
Secondary	1.000 A	0A.13
T2 CT		0A.14
Polarity	Standard	0A.15
Primary	1200 A	0A.16
Secondary	1.000 A	0A.17

Table 3. Auto transformer implementation in relay.

CT and VT Ratios	Value	Address (C.R)
Winding Type	Auto	30.02
HV CT Terminals	01	30.03
LV CT Terminals	10	30.04
Ref Power S	160.0 MVA	30.07
HV Connection	Y-Wye	30.08
HV Grounding	Grounded	30.09
HV Nominal	220.0 kV	30.0A
HV Rating	160.0 MVA	30.0B
Percentage Reactance	25.00%	30.0C
LV Vector Group	0	30.0D
LV Connection	Y-Wye	30.0E
LV Grounding	Grounded	30.0F
LV Nominal	132.0 kV	30.10
LV Rating	160.0 MVA	30.11
Match Factor CT1	2.858	30.20
Match Factor CT2	1.715	30.21
Phase Sequence	Standard ABC	30.5E

Table 3 corresponds to auto transformer data implemented in the differential relay. Power rating of both HV and LV winding is set to 160 MVA. The HV and LV connection of the auto transformer are in 'Y'. The HV nominal voltage rating and LV nominal voltage rating are 220 and 132 kV, respectively. The neutral of HV and LV winding is considered as 'grounded'. Figure 4 shows the graphical differential characteristics or bias characteristics implemented for the testing. The setting 'Trans Diff' is set to 'enabled', which means that the differential protection function is enabled in the relay. In Table 4 and Figure 4, the current I_{S1} is pick-up setting of the differential relay. Setting 'K1' in Table 4 and Figure 4 is the percentage slope for the slope 2 of differential characteristics. The slope provides restraining of differential protection operation in case of spill current occurrence due to the tap changing operation, CT errors, and through faults. The differential relay must remain stable and must not initiate tripping during through faults. However, the CT errors may result in larger mismatched current or spill current or differential current as defined in Figure 2b, which depends on fault intensity. In such cases, the restraining to differential operation is provided through slope setting 'K1 = 30%'. Slope is the ratio of change in differential current to the change in bias current.
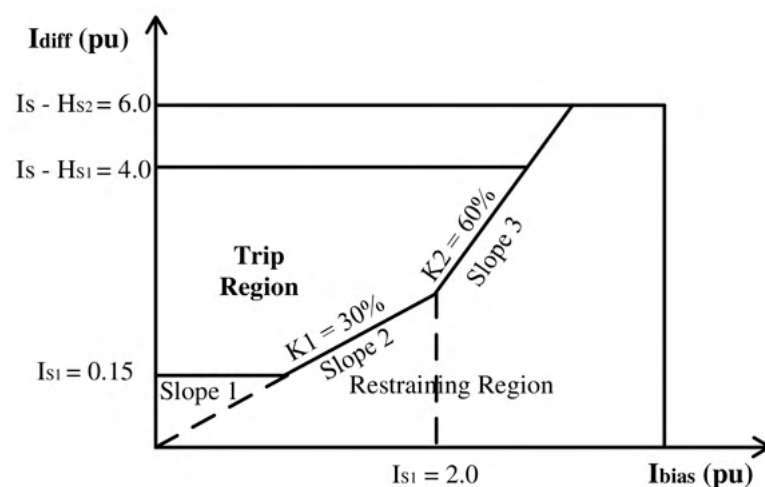

Figure 4. Differential characteristics or bias characteristics implemented in relay.

Table 4. Differential protection settings implementation in relay.

CT and VT Ratios	Value	Address (C.R)
Trans Diff	Enabled	31.01
Set Mode	Advanced	31.02
I_{S1}	150×10^{-3} PU	31.03
K1	30.00%	31.04
I_{S2}	2.000 PU	31.05
K2	60.00%	31.06
tDIFF LS	0 s	31.07
$I_S - CTS$	250×10^{-3} PU	31.08
$I_S - H_{S1}$	4.000 PU	31.10
H_{S2} Status	Enabled	31.11
$I_S - H_{S2}$	6.000 PU	31.12
Zero seq. filt. HV	Enabled	31.20
Zero seq. filt. LV	Enabled	31.21
2nd harmonic blocked	Enabled	31.28
I_h (2)% >	15.00%	31.29
Cross blocking	Enabled	31.2A
CT-Sat and No-Gap	Enabled	31.2B
5th harmonic blocked	Enabled	31.33
I_h (5)% >	40.00%	31.34
Circuitry fail	Disabled	31.40

In Table 4, the setting I_{S2} marks the start of slope 3, as shown in Figure 4. The slope 3 provides restraining of differential protection, during through fault, even if the main CT is saturated. The setting 'K2' in Table 4 and Figure 4 defines the percentage slope setting for slope 3. The setting '$I_S - H_{S1}$' in Table 4 and Figure 4 monitors the operational peak of the differential current. Beyond setting '$I_S - H_{S1}$', the 2nd harmonic restrain cannot restrain differential relay operation. Therefore, the setting should be kept higher than expected peak magnetizing current. Setting '$I_S - H_{S1}$' only results in tripping if the peak value of the differential current exceeds '$I_S - H_{S1}$' setting and operating point lies in trip region of the bias characteristics. If differential current exceeds the setting '$I_S - H_{S2}$', as shown in Table 4 and Figure 4, the differential relay causes tripping regardless of biasing characteristics and harmonic components. The differential relay continuously calculates I_{diff} and I_{bias} current through HV and LV secondary currents at its terminals. If the calculated I_{diff} and I_{bias} currents end up in the tripping region, the differential relay will initiate tripping as per the defined algorithm. Setting 'Zero sequence filtering, HV' and 'Zero sequence filtering LV' set to 'Enabled' will result in the elimination of zero sequence current components through HV and LV MCTs. The 2nd, 5th harmonic blocking are set at 15% and 40%, respectively.

6. Testing of Differential Relay

6.1. Test Apparatus

Testing of the differential relay is conducted through a six current source secondary injection universal relay test set connected to the relay, as shown in Figure 5a,b. The settings and configuration of the relay is performed through S1 Agile Software, and the computer is used for reference setting and result monitoring. The relay trip contact is used as stop contact for the test set.

6.2. Measurement Test

A measurement test is performed to ascertain that the relay is reading the current at its terminals accurately. Through the measurement test, the correctness of CT ratios and measurement of differential and restraining current is determined (in pu). The nominal current or full load current at primary and secondary side of the transformer is calculated using Equation (1) as $I_{nom.pri} = 420$ A and $I_{nom. sec} = 700$ A. The CT ratio at primary and secondary side of the transformer is computed as [4]:

$$\text{CT Ratio} = \frac{\text{Rated Primary Current}}{\text{Rated Secondary Current}} = \frac{1200}{1} = 1200 \tag{2}$$

$$I_{\text{nom.pri. sec}} = \frac{I_{\text{nom.pri}}}{\text{CT Ratio}} = \frac{420}{1200} = 0.35 \tag{3}$$

$$I_{\text{nom. sec . sec}} = \frac{I_{\text{nom. sec}}}{\text{CT Ratio}} = \frac{700}{1200} = 0.58 \tag{4}$$

Referring to Figure 2b, the differential current is computed as vector sum of currents flowing through it as [4]:

$$I_{\text{diff}} = \left| \vec{I_1} + \vec{I_2} \right| \tag{5}$$

where I_1 and I_2 are the secondary current of HV MCT and LV MCT, respectively, that are shown as I_A and I_B in Figure 2b. The $\vec{I_1}$ and $\vec{I_2}$ are vector quantity currents flowing in the differential coil. Restraining current or bias current provides restrain to the differential relay operation [26]. The bias current is based on the loading of the transformer and hampers the operation of the relay. However, the bias current computation in differential relay differs in different makes and models, and even the same manufacturer may have different mathematical equation for its computations. Bias current is computed in Equation (6) as follows [4]:

$$I_{\text{bias}} = \frac{|I_1| + |I_2|}{2} \tag{6}$$

Both the differential and bias currents are measured as per unit quantities, where per unit value is the ratio of actual and base values. The base value is the rated secondary current of the main CTs that in our case is taken as 1A. Whereas, the HV MCT ratio and LV MCT ratio are automatically calculated by differential relay as 2.858 and 1.715, respectively, using Equation (7) [4].

$$\text{HV MCT Ratio or LV MCT Ratio} = a = \frac{I_{\text{sec ondary}}}{I_{\text{primary}}} \tag{7}$$

Referring to Figure 6a and using HV MCT Ratio, we can illustrate that upon the injection of balanced three phase nominal HV secondary current ($0.35A$) into corresponding relay current elements with no current injection into LV side relay current elements, current equal to 1A flows in secondary of HV MCT, resulting in flow of $I_{diff} = 1$ pu using Equation (5) and $I_{bias} = 0.5$ pu using Equation (6). In Figure 6a, the phase shift of three phases is shown through clock convention, where 0 corresponds to 0°, 4 corresponds to $-120°$, and 8 corresponds to $-240°$. Therefore, in order to thoroughly verify the HV side relay elements measurement, HV secondary current corresponding to the different loading conditions is simulated and then by computing HV primary current values. Moreover, the differential current and bias current are compared with observed values. Tables 5 and 6 record the measurement results of the HV side relay current elements. Referring to Figure 6b and LV MCT Ratio, the injection of balanced three phase nominal LV secondary current (0.58A) into corresponding relay current elements with no current injection into HV side relay current elements, the current equal to 1A flows in secondary of the LV MCT, resulting in flow of $I_{\text{diff}} = 1$ pu using Equation (5) and $I_{\text{bias}} = 0.5$ pu using Equation (6). In Figure 6b, the clockwise phase shift of three phases is shown, where 6, 10, and 2 correspond to $-180°$, $-300°$, and 60°. Tables 5 and 6 record the measurement results of the LV side relay current elements.
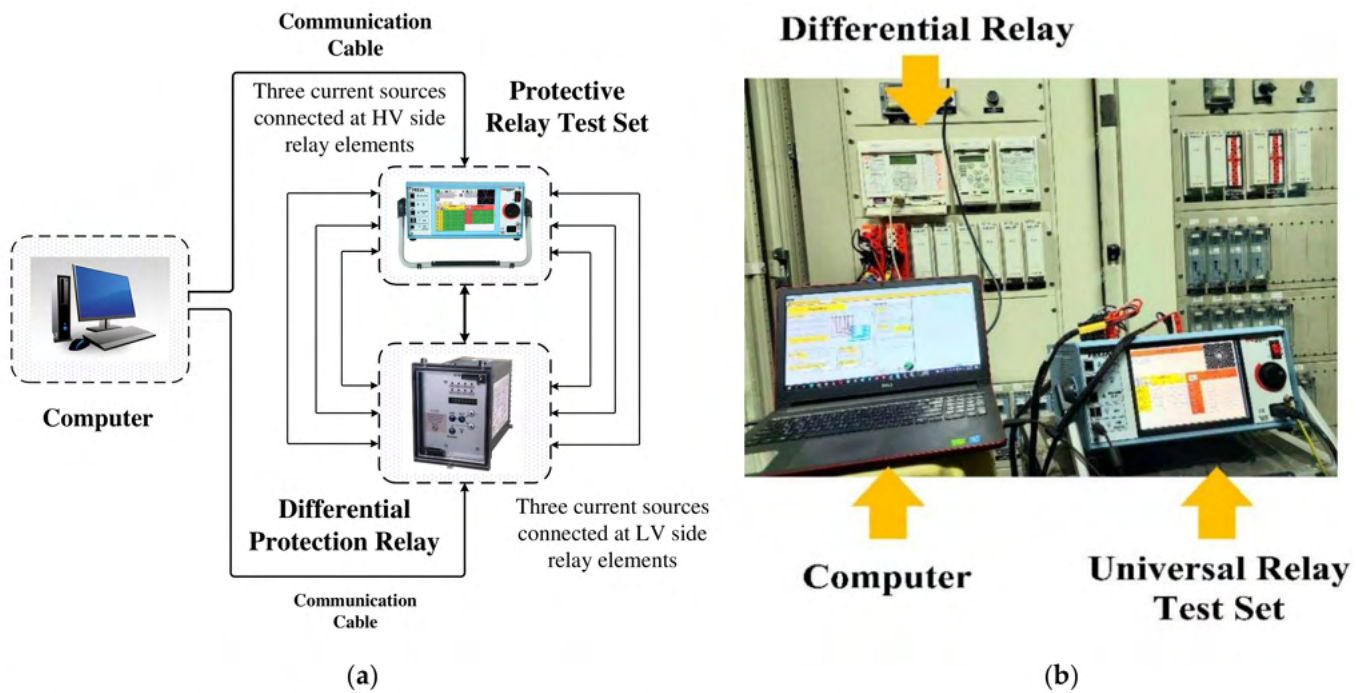
Figure 5. Test bench with differential relay, test set, and computer: (**a**) schematic diagram, (**b**) pictorial view of hardware setup.
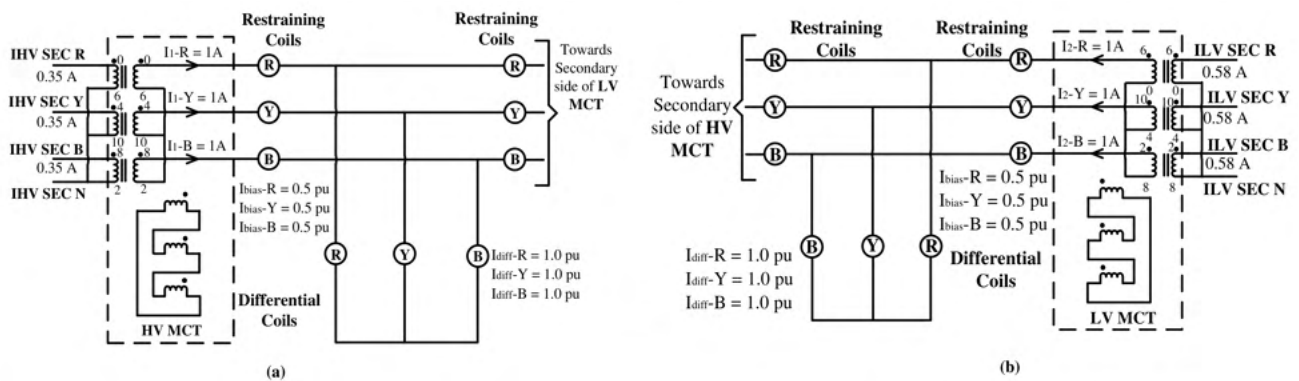

Figure 6. Three phase balanced current injection and resulting differential and bias currents in per unit (pu) for: (**a**) HV nominal secondary and (**b**) LV nominal secondary.

Table 5. Primary current observed by relay for different percentage loading of: (**A**) transformer HV side in terms of HV secondary current and (**B**) transformer LV side in terms of LV secondary current.

Percentage Loading	(A) Transformer HV Side					(B) Transformer LV Side				
	HV Sec. Current (A)	Calc. HV Primary Current (A)	Obs. HV Primary (A)			LV Sec. Current (A)	Calc. LV Primary Current (A)	Obs. LV Primary (A)		
20%	0.07	84	84.4	84.3	84.7	0.116	139.92	140.8	140.5	141
40%	0.14	168	169.7	168.5	169.1	0.2332	279.84	280.1	280.7	281.3
60%	0.21	252	252.6	254.1	253.1	0.3498	419.76	421	421.8	421.1
80%	0.28	336	338.1	340.2	339.8	0.4664	559.68	564	564.4	564.3
100%	0.35	420	421.9	424.3	422.2	0.583	699.6	707.9	706.7	706.3

Table 6. Differential and bias current measured by relay for different percentage loading of: (**A**) transformer HV side and (**B**) transformer LV side.

Percentage Loading	(A) Transformer HV Side				(B) Transformer LV Side			
	Differential Current (pu)		Bias Current (pu)		Differential Current (pu)		Bias Current (pu)	
	Calc.	Obs. (Avg)	Calc	Obs.	Calc.	Obs. (Avg)	Calc.	Obs.
20%	0.2	0.201	0.1	0.101	0.2	0.202	0.1	0.102
40%	0.4	0.406	0.2	0.202	0.4	0.404	0.2	0.202
60%	0.6	0.608	0.3	0.303	0.6	0.603	0.3	0.302
80%	0.8	0.811	0.4	0.405	0.8	0.809	0.4	0.403
100%	1	1.01	0.5	0.505	1	1.02	0.5	0.506

6.3. Pickup Test

A pickup test is performed to check the setting I_{S1} in differential relay and conducted separately from HV side and LV side relay elements. From Figure 6a, the pickup computes the minimum differential current that initiate relay tripping. For pickup test, Equations (8) and (9) compute the 3-phase HV side and LV side secondary currents related the pickup setting *Is*1 [5]. By injecting the secondary current (Equation (8)) to the HV side while keeping LV side to zero, the relay should pick up and trip as per setting. Similarly, if the current (Equation (9)) is injected to the LV side relay elements, the relay should pick up and tripping as per setting while keeping HV side to zero. The $HV_{nom\ sec}$ and $LV_{nom\ sec}$ are the nominal secondary CT currents for HV and LV sides.

$$3 - Phase\ Pickup\ current\ for\ HV\ side = I_{S1} \times HV_{nom\ sec} \qquad (8)$$

$$3 - Phase\ Pickup\ current\ for\ LV\ side = I_{S1} \times LV_{nom\ sec} \qquad (9)$$

During testing, the gradual current increase is observed till relay pick up threshold and compared with the calculated value. Moreover, the respective current is gradually decreased until the relay drops off. Equations (10) and (11) are used for single phase pickup current injection calculation for HV and LV sides, respectively, while Equations (12) and (13) are used for two phase pickup current injection calculation for HV and LV sides, respectively [5].

$$1\ Ph.\ Pickup\ current\ for\ HV\ side = I_{S1} \times HV_{nom\ sec} \times MF \qquad (10)$$

$$1\ Ph.\ Pickup\ current\ for\ LV\ side = I_{S1} \times LV_{nom\ sec} \times MF \qquad (11)$$

$$2\ Ph.\ Pickup\ current\ for\ HV\ side = I_{S1} \times HV_{nom\ sec} \qquad (12)$$

$$2\ Ph.\ Pickup\ current\ for\ LV\ side = I_{S1} \times LV_{nom\ sec} \times MF \qquad (13)$$

where MF is the multiplying factor where applicable that depends on the MCT configuration and zero sequence current filtering (enabled or disabled) status. For Equations (10)–(13), the *MF* is computed using sequence current (I_0, I_1, and I_2) given in Ref. [5]. Using [5], it is apparent that *MF* value in Equations (10) and (11) is $\frac{3}{2}$, while in Equation (13) the *MF* is 1. Table 7 shows the single, double, and three phase testing results where the acceptable range for pick-up observed is computed using the following range formula given in [24] as $0.9 \times Pickup\ Calc. - 1.1 \times Pickup\ Calc$, and for drop-off observed, the range I defined as $0.9 \times Pickup\ Calc.$ to $1.0 \times Pickup\ Calc$. Table 7 illustrates that for both HV and LV sides, all the pickup observed, and drop-off observed values for single, double, and three phase pickup tests are within the aforementioned ranges.

Table 7. Single, double, and three phase pickup and drop-off test of differential relay.

Sr. No.	HV Side			LV Side		
	Pickup Calc. (A)	Pickup Obs. (A)	Drop off Obs. (A)	Pickup Calc. (A)	Pickup Obs. (A)	Drop off Obs. (A)
Single Phase Pickup Test						
R	0.078	0.078	0.073	0.131	0.133	0.123
Y	0.078	0.079	0.074	0.131	0.131	0.122
B	0.078	0.08	0.072	0.131	0.130	0.124
Double Phase Pickup Test						
RY	0.0525	0.052	0.048	0.0874	0.087	0.082
YB	0.0525	0.051	0.047	0.0874	0.087	0.081
BR	0.0525	0.051	0.048	0.0874	0.086	0.081
Three Phase Pickup Test						
RYB	0.0525	0.052	0.048	0.0874	0.088	0.082

Figure 7a shows the waveform for HV side Blue phase (IC_1) observed pickup current (0.08 A)). Before the injection of observed pickup current, transformer rated currents are applied as pre-fault to the differential relay. The pre-fault current values read by relay are 419.6 A (RMS) for primary side and 698.6 A (RMS) for secondary side. The fault current in IC_1 measured by relay is 105.5 A (RMS), secondary current $= \frac{105.5}{1200} = 0.087$ A). The injected secondary current generates $I_{diff} = 0.149$ according to graph which is very close to the pickup setting of relay (0.15 pu).

Figure 7b shows the waveform for LV side yellow phase (IB_2) observed pickup current (0.131 A). Before the injection of observed pickup current, transformer rated currents are applied as pre-fault to differential relay. The pre-fault current values read by relay are 421.9 A (RMS) for primary side and 693.9 A (RMS) for secondary side. The fault current in IB_2 measured by relay is 168.7 A (RMS), secondary current $= \frac{168.7}{1200} = 0.140$ A). The injected secondary current generates $I_{diff} = 0.149$ as per graph, which is very close to the pickup setting of relay (0.15 pu).

Figure 7c shows the waveform for HV side three phase (IA_1, IB_1, IC_1) observed pickup current (0.052 A). Before the injection of observed pickup current, transformer rated currents are applied as pre-fault to differential relay. The pre-fault current values read by relay are 417.3 A (RMS) for primary side and 696.2 A (RMS) for secondary side. The fault currents IA_1, IB_1, IC_1 measured by relay are 69.78 A (RMS), secondary current $= \frac{69.78}{1200} = 0.058$ A. The injected secondary current generates $I_{diff} = 0.149$ as per graph, which is close to pickup setting of relay (0.15 pu).

Figure 7d shows the waveform for LV side three phase (IA_2, IB_2, IC_2) observed pickup current (0.088 A). Before the injection of observed pickup current, transformer rated currents are applied as pre-fault to differential relay. The pre-fault current values read by relay are 414.9 A (RMS) for primary side and 698.5 A (RMS) for secondary side. The fault current IA_2, IB_2, IC_2 measured by relay is 103.15 A (RMS), secondary current $= \frac{103.15}{1200} = 0.085$ A). The injected secondary current generates $I_{diff} = 0.151$ as per graph, which is close to pickup setting of relay (0.15 pu).

6.4. Trip Time Test

The trip time test is performed to measure the time from inception of fault till relay trips. The recommendation is to test trip time at $5.0 \times HV\ Pickup\ Calc.$ [24]. The results of trip time test are recorded using three-phase current injection into HV side relay current elements $5.0 \times HV\ Pickup\ Calc.$, which is 0.2625 A. The acceptable range is 30–35 ms, while observed is 27 ms. The simulation and analysis performed in Section 6.9 explicitly discuss the trip time test of numerical differential relay.
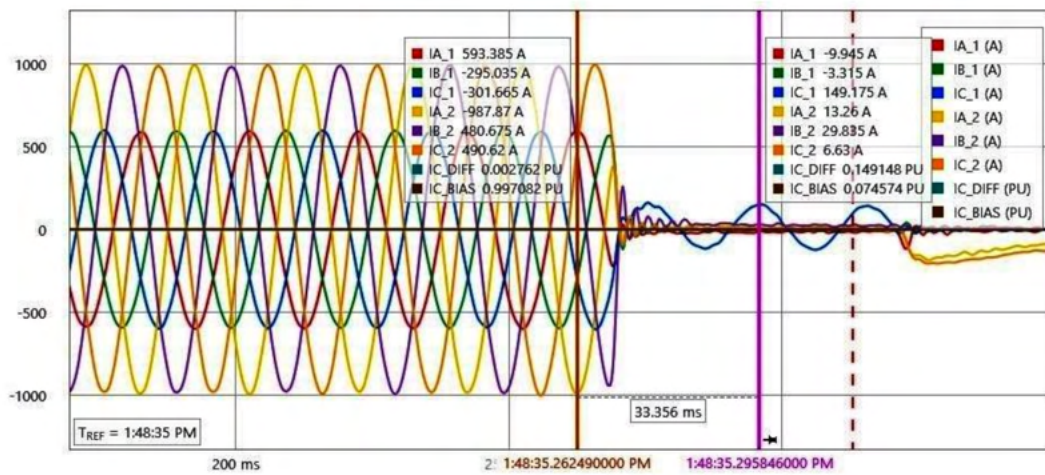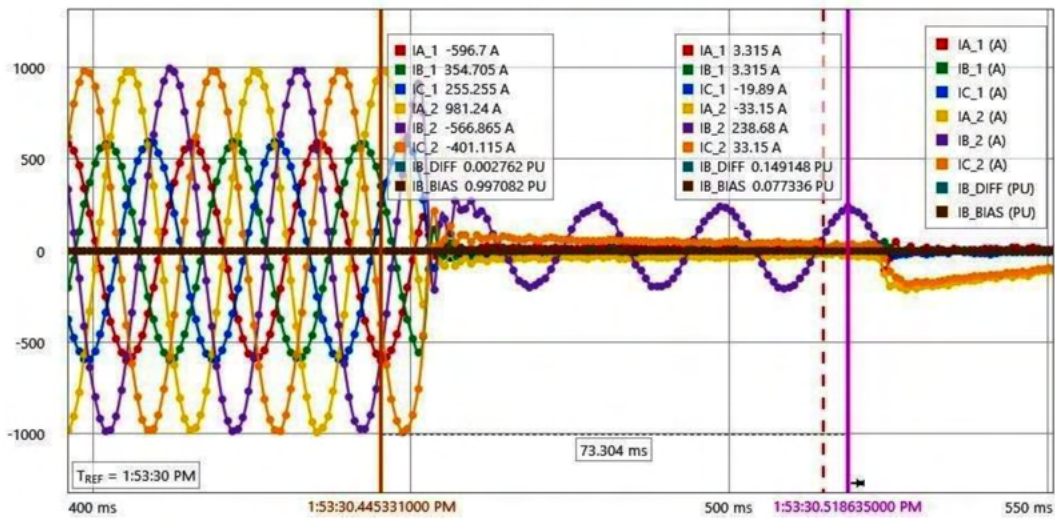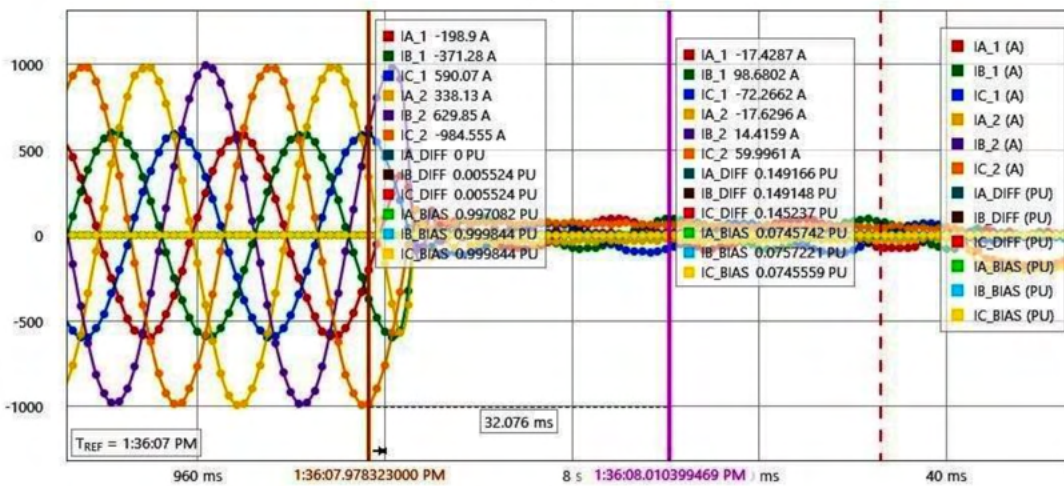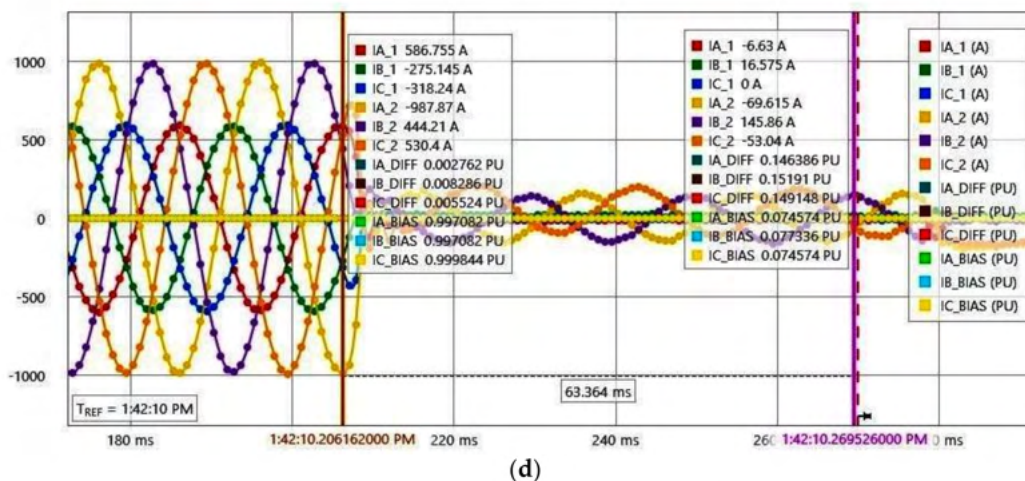
Figure 7. *Cont.*

Figure 7. Pickup and drop-off test of differential relay: (**a**) HV side blue phase, (**b**) LV side yellow phase, (**c**) HV side three phase, (**d**) LV side three phase.

6.5. Stability Test

During through fault, the relay must remain stable and must not initiate tripping. Ideally, the bias current increases but the differential current remains low (near to zero). Practically, some differential current may be observed (due to CT saturation); however, the relay remains stable due to bias characteristics. The stability test is performed by simulating the condition for through fault. The condition can be simulated by simultaneously applying nominal HV and LV secondary currents at respective relay current elements. Table 8 presents the differential and bias currents measurements by the relay when 5 times of balanced HV and LV nominal secondary currents are applied at relay terminals.

6.6. Bias Test

Referring to the bias characteristics shown in Figure 4, testing of bias characteristics includes testing all three slopes. For each slope, two points are considered on the graph, near to the boundary of trip and restrain region. The current injections that correspond to the selected points are injected in the relay and its behavior is recorded. Figure 8 shows the points selected on Figure 4. Using Equations (5) and (6), the currents I_1 and I_2 shown in Figure 6a,b, respectively, are calculated for each point selected on Figure 8. Moreover, the $I_{HV\ sec}$ and $I_{LV\ sec}$ corresponding to I_1 and I_2, respectively, are calculated in amperes. The 3-phase $I_{HV\ sec}$ and $I_{LV\ sec}$ with angles shown in the stability test are applied simultaneously to the corresponding relay elements. The behavior of relay (Trip/No Trip) is recorded, and I_{diff} and I_{bias} measured by relay is compared with the computed value of selected point. To illustrate this phenomenon, recorded results are shown in Table 9.

Figure 9a shows the waveform of currents corresponding to Point 'B' mentioned in Table 9. Before the injection of currents corresponding to Point 'B', transformer rated currents are applied as pre-fault to differential relay. The pre-fault current values read by relay are 414.9 A (*RMS*) for primary side and 698.6 A (*RMS*) for secondary side. The injected three phase HV and LV fault currents into relay result into $I_{diff} = 0.18$ pu and $I_{bias} = 0.40$ pu. The observed I_{diff} and I_{bias} from relay are in accordance with the I_{diff} and I_{bias} of Point 'B' as apparent from Figure 8.

Figure 9b shows the waveform of currents corresponding to Point 'F' mentioned in Table 9. The injected three phase HV and LV fault currents into relay result into $I_{diff} = 1.26$ pu and $I_{bias} = 3.0$ pu. The observed I_{diff} and I_{bias} from relay are in accordance with the I_{diff} and I_{bias} of Point 'F' as apparent from Figure 8.

Point A : (0.4 , 0.12)
Point B : (0.4 , 0.18)
Point C : (1.2 , 0.33)
Point D : (1.2 , 0.39)
Point E : (3.0 , 1.15)
Point F : (3.0 , 1.25)
Point G : (10 , 5.2)
Point H : (10 , 5.6)
Point I : (12 , 6.4)
Point J : (12 , 6.8)

Figure 8. Differential characteristics or bias characteristics with selected points.

6.7. The 2nd and 5th Harmonic Restraint Test

6.8. High Stage 1 and High Stage 2 Test

$I_{diff} = 6.4$ pu & $I_{bias} = 12.0$ pu. The observed I_{diff} and I_{bias} from relay are in accordance with the I_{diff} and I_{bias} of Point 'I' as apparent from Figure 8.

Table 9. Test results of bias characteristics for points selected in Figure 11a.

Point	I_1(pu)	I_2(pu)	$I_{HV\,sec}$(A)	$I_{LV\,sec}$(A)	I_{diff} obs. (pu)	I_{bias} obs. (pu)	Trip/No Trip
A	0.46	0.34	0.161	0.198	0.12	0.404	No trip
B	0.49	0.31	0.171	0.180	0.18	0.404	Trip
C	1.36	1.03	0.478	0.603	0.33	1.213	No trip
D	1.39	1.00	0.488	0.586	0.39	1.213	Trip
E	3.57	2.42	1.251	1.413	1.16	3.028	No trip
F	3.62	2.37	1.269	1.384	1.26	3.031	Trip

Table 10. Results of 2nd and 5th harmonic restraint test.

Relay Current Element	Current Injected (A) 50 Hz	2nd Harm. Block Th. Setting (%)	2nd Harm. Block Obs.%	5th Harm. Block Th. Setting%	5th Harm. Block Obs.%
$I_{HV\,sec\,R}$	0.5	15	14.6	40	41.1
$I_{HV\,sec\,Y}$	0.5	15	14.6	40	40.9
$I_{HV\,sec\,B}$	0.5	15	14.2	40	40.4

Table 11. Test results of effect of setting '$I_S - H_{S1}$' and 2nd harmonic component on differential protection status.

HV Side Relay Element	I_{diff} (per Unit)	Current Applied (A) (50 Hz)	2nd Harmonic Current	Differential Protection Status
Red	3.6	1.9	14.7%	Blocked
	4.10	2.16	≥14.7%	Unblocked
Yellow	3.6	1.9	14.8%	Blocked
	4.10	2.16	≥14.8%	Unblocked
Blue	3.6	1.9	14.8%	Blocked
	4.10	2.16	≥14.8%	Unblocked

Table 12. Test results of bias characteristics for points selected in accordance with setting '$I_S - H_{S1}$' and '$I_S - H_{S2}$' in Figure 11a.

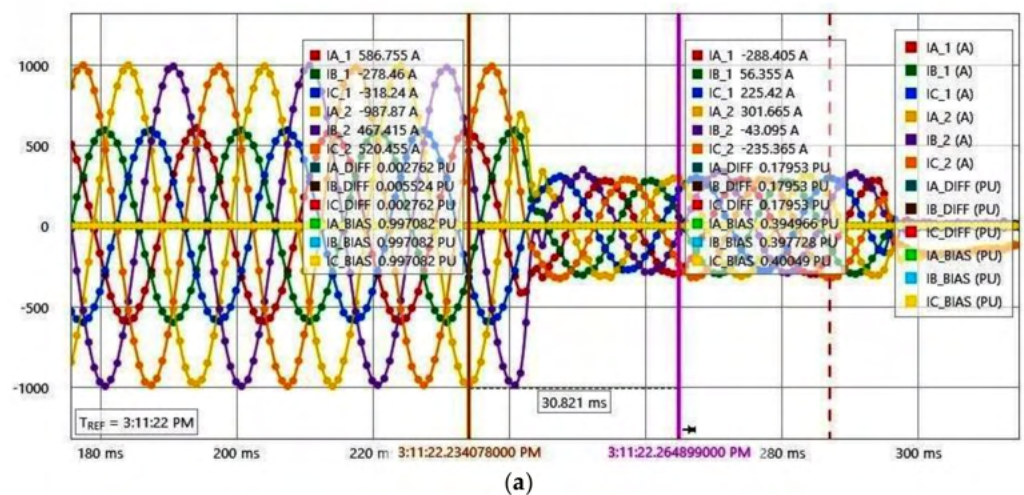| Point	I_1(pu)	I_2(pu)	$I_{HV\,sec}$(A)	$I_{LV\,sec}$(A)	I_{diff} Obs. (pu)	I_{bias} Obs. (pu)	Trip/No Trip
G	12.6	7.4	4.41	4.31	5.23	10	No Trip
H	12.8	7.2	4.48	4.19	5.63	10.0	Trip
I	15.2	8.8	5.32	5.13	6.44	12	Trip
J	15.4	8.6	5.39	5.01	6.84	12	Trip

Figure 9. *Cont.*
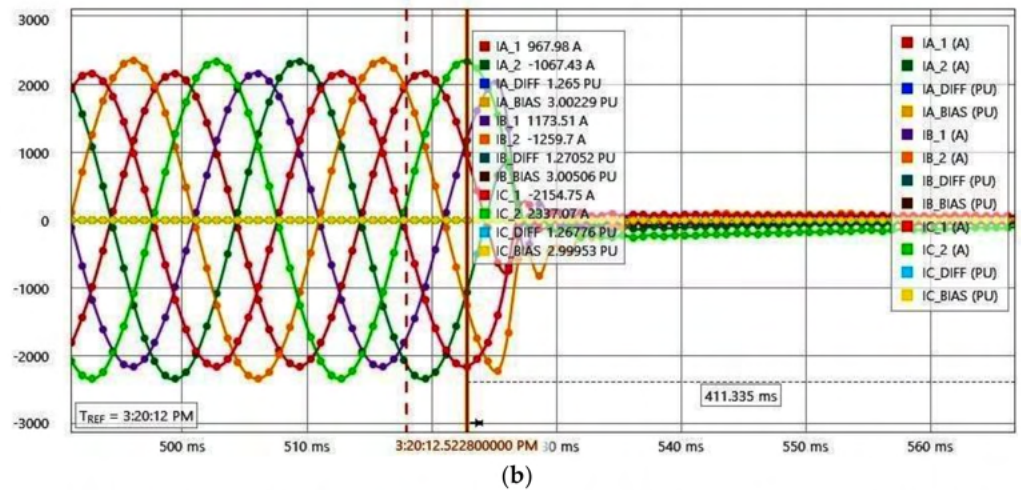
(b)

Figure 9. Waveforms of bias characteristics for points selected in Figure 11a: (**a**) point B, (**b**) point F.
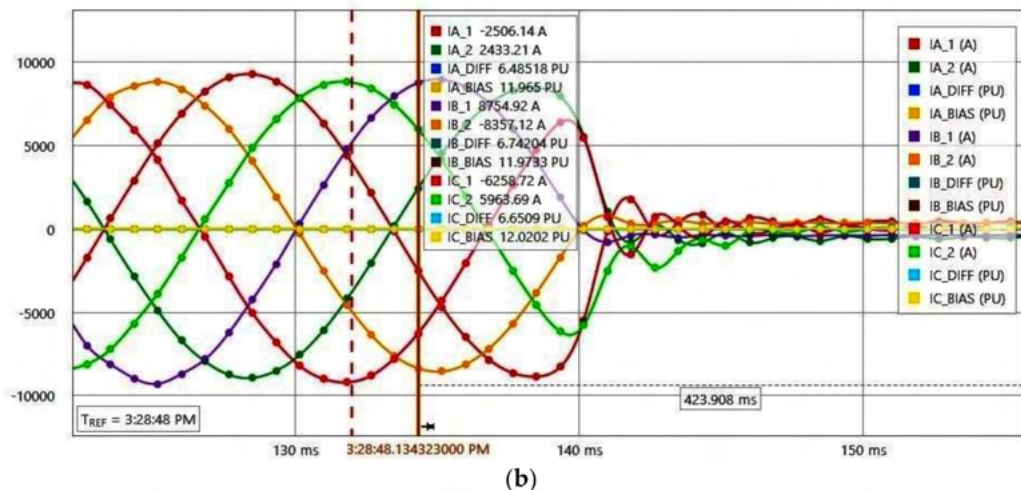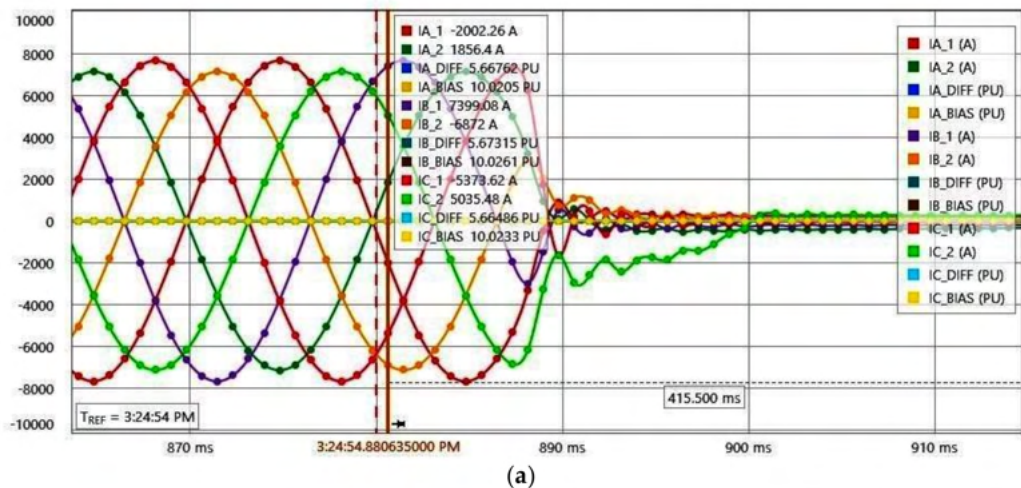

(a)

(b)

Figure 10. Waveforms of bias characteristics for points selected in accordance with setting '$I_S - H_{S1}$' and '$I_S - H_{S2}$' in Figure 11a: (**a**) point H, (**b**) point I.

6.9. Simulation Results and Discussion

In addition to testing, the numerical relays also generate time stamped waveforms and measurements as standard format COMTRADE [27]. Such waveform can provide important insight into pre-fault conditions, fault inception, post-fault conditions, and behavior of relay under real-time fault situations. Few current waveforms from COMTRADE files

generated by relay for trip time test and bias characteristics test (point D) are displayed for discussion. Current waveforms for trip time test (fault current applied for extended time regardless of relay trip) and bias characteristic test at point D (fault current applied with nominal currents as pre-fault) in Figure 8 are presented in Figures 8a and 11b, respectively. The waveforms are plotted through SEL SynchroWAVE Event [28]. Figure 11a shows relay reads Red Phase Primary Current (IA_1_1.sec) as $307A$ (RMS), which is approximately equal to $315A$, as per discussed calculations. Similarly, Red Phase Differential Current (IA_DIFF) is observed as $I_{diff} = 0.7540$ pu and Red Phase Bias Current (IA_BIAS) is observed as $I_{bias} = 0.3783$ pu. Observed values of Red Phase Differential Current (IA_DIFF) and Red Phase Bias Current (IA_BIAS) are as per calculations discussed. The calculated values of Red Phase Differential Current and Red Phase Bias Current being $I_{diff} = 0.75$ pu and $I_{bias} = 0.375$ pu, respectively. Figure 11b shows transformer red phase currents calculated by relay (IA_1_1.sec corresponds to HV side red phase current, IA_2_1.sec corresponds to LV side red phase current, IA_DIFF corresponds to red phase differential current, and IA_BIAS corresponds to red phase bias current) when point D in Figure 8 is simulated with nominal currents as pre-fault. The brown and purple color cursor shows HV side, LV side, I_{diff} and I_{bias} currents of red phase at pre-fault and fault values, respectively. Pre-Fault Red Phase Primary currents of HV side and LV side calculated by relay are 440A (RMS) and 690A (RMS), respectively. The calculated primary current values are close to actual nominal current of HV side (420A) and LV side (700A). During pre-fault, I_{diff} and I_{bias} currents of red phase are calculated by relay as $I_{diff} = 0.008$ pu and $I_{bias} = 1.010$, respectively. Pre-fault values of I_{diff} and I_{bias} calculated by relay are very close to actual calculated values of I_{diff} and I_{bias} given as $I_{diff} = 0$ pu and $I_{bias} = 1.0$ pu. Fault values of I_{diff} and I_{bias} calculated by relay, shown in Figure 11b, are $I_{diff} = 0.3949$ pu and $I_{bias} = 1.2263$. Fault values of I_{diff} and I_{bias} calculated by relay are very close to actual calculated values of I_{diff} and I_{bias} for point D given as $I_{diff} = 0.39$ pu and $I_{bias} = 1.2$ also shown in Figure 8.
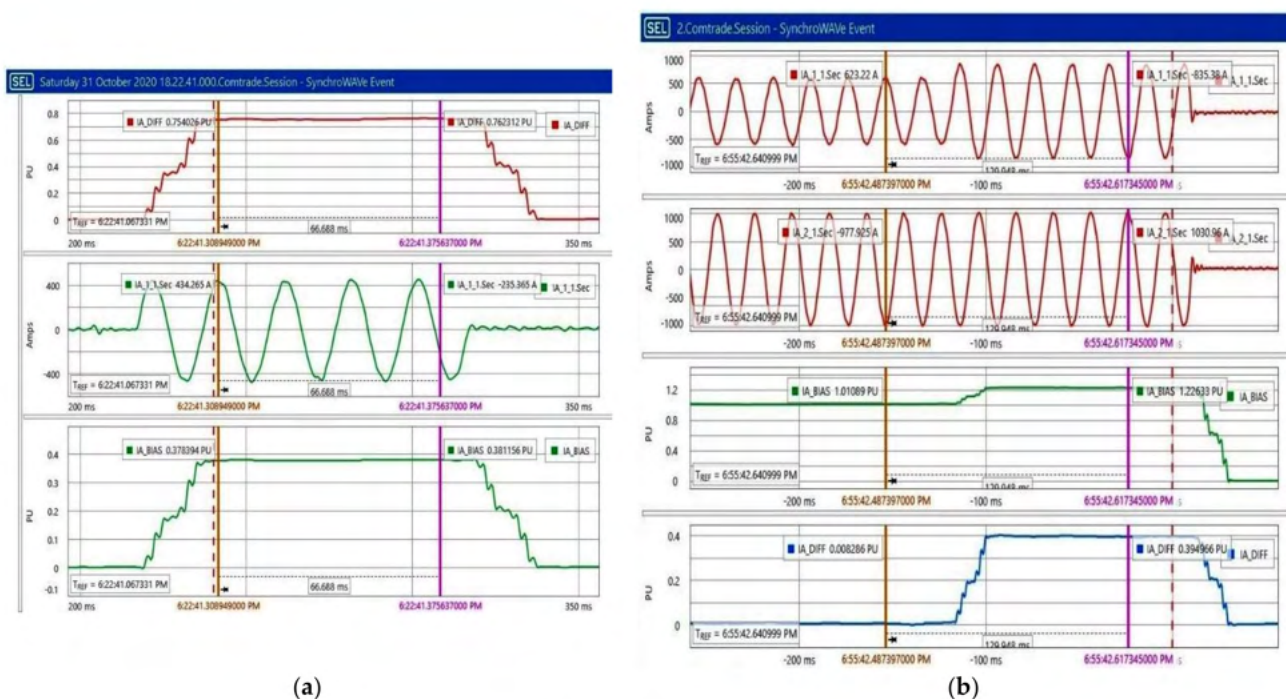

Figure 11. Waveform of: (**a**) Red Phase Current, I_{diff} and I_{bias} of red phase for fault simulated in trip time test, (**b**) HV and LV Red Phase Current, I_{diff} and I_{bias} for point D of Figure 8.

7. Conclusions and Future Work

In this paper, a complete procedural guideline for the practical implementation of numerical differential relay testing procedures was prepared and composed for insight analysis of relay settings for the protection of an EHV 220/132 kV auto transformer. Moreover, based on the experimental results, a detailed technical and theoretical analysis including connection details, operating principle, and biasing characteristics was also performed. A secondary injection relay test set was used for the detailed testing of numerical differential relay. For this purpose, a "six current source secondary injection universal relay test set" was connected to the relay. Keeping in view of the prepared formal procedural guideline, the real-time implementation of relay was performed, which gives a detailed insight study that can be helpful for the research community and power system protection experts in understanding the basic principles, operation, and testing of numerical differential relays. The tests used to monitor a relay's health include measurement test, pickup test, trip-time test, stability test, bias characteristics test, 2nd and 5th harmonic restraints test, and high stage 1 and high stage 2 test. The testing results were then critically analyzed from theoretical and practical perspectives to insure the relay's satisfactory performance. Table 13 tabulates the summarized results of relay testing with the final remarks presented against each test. The testing results of the differential relay under consideration are satisfactory and indicate the sound health and appropriate functionality of relay.

Table 13. Summarized results of differential relay testing.

Sr. No.	Test Performed	Observations	Remarks
1	Measurement Test	Comparison of meas. and calc. values	Satisfactory
2	Pickup Test	Single, double, and three phase pickup test results lie in acceptable range specified in [24]	Satisfactory
3	Trip Time Test	The observed trip time lies in acceptable range (30 to 35 ms) specified in [24]	Satisfactory
4	Stability Test	Observed I_{diff} and I_{bias} values are comparable to calc. values	Satisfactory
5	Bias Characteristics Test	Bias characteristics test result for test points shown in Figure 8 are as per respective region (trip/restrain). Additionally, the obs. I_{diff} and I_{bias} currents of relay are comparable to calc. I_{diff} and I_{bias} shown in Figure 8.	Satisfactory
6	2nd and 5th Harmonic Restraint Test	Observed 2nd and 5th harmonic restraint test results are comparable to the corresponding setting thresholds	Satisfactory
7	High Stage 1 and High Stage 2 Test	High Stage 1 and 2 test results for test points shown in Figure 8 are as per respective region (trip/restrain)	Satisfactory

If the behavior of relay deviates from the applied settings in such a way that the deviation is greater than the allowed tolerance by manufacturer and it is made sure again that the testing procedure followed is proper and comprehensive and the relay settings under test are properly understood by testing engineer, then proceedings can be made to declare the relay unhealthy. Moreover, diagnosis can also be made through testing to determine whether any analogue, input/output module, CPU module, or power supply module is faulty. After identification and replacing the faulty module with the healthy one, the relay is to be tested again to ensure its healthiness.

In future, a detailed manual will be prepared which will include comprehensive testing procedural guidelines for understanding the complex design, features, and working of the numerical distance protection relay used for the protection of EHV transmission lines.

Author Contributions: Conceptualization, U.E., M.J. and U.J.; methodology, K.S.Z., A.U.R. and A.R.; validation, M.M.A., H.H. and M.S.; formal analysis, U.E., M.J. and U.J.; investigation M.M.A., H.H. and M.S.; resources, K.S.Z., A.U.R. and A.R.; data curation, M.M.A., H.H. and M.S.; writing—original draft preparation, U.E., M.J. and U.J.; writing—review and editing, M.M.A., H.H. and M.S.; visualization, K.S.Z., A.U.R. and A.R.; supervision, K.S.Z., A.U.R. and A.R.; project administration M.M.A., H.H. and M.S. All authors have read and agreed to the published version of the manuscript.

References

1. Bak, C.L.; Hansen, M.L.; Nissen, J.O. Distance protection in 150/60 kV transformer 60 kV feeders: Two real blackout case studies. *J. Eng.* **2018**, *2018*, 802–806. [CrossRef]

2. Khan, S.S.; Mehmood, K.T.; Hashmi, M.W.; Rafiq, M.A.; Sheikh, M.F. Power stability of 500/220/132 kV grid station system on single-line-to-ground fault at 500 kv transmission lines. *Sci. Int. J.* **2015**, *27*, 3995–3999.

3. Akhmedova, O.; Soshinov, A.; Gazizov, F.; Ilyashenko, S. Development of an Intelligent System for Distance Relay Protection with Adaptive Algorithms for Determining the Operation Setpoints. *Energies* **2021**, *14*, 973. [CrossRef]

4. Verzosa, Q.; Lee, W.A. Testing Microprocessor-Based Numerical Transformer Differential Protection. *IEEE Trans. Ind. Appl.* **2017**, *53*, 56–64. [CrossRef]

5. Rocha, D.C.G.; Batista, W.H.; Coelho, A.L.M.; Araujo, M.R. Practical approach to testing the transformer differential protection for internal and external faults, CT saturation and inrush transients. *J. Eng.* **2018**, *2018*, 1239–1244. [CrossRef]

6. Andreev, M.; Suvorov, A.; Ruban, N.; Ufa, R.; Gusev, A.; Askarov, A.; Kievets, A.; Bhalja, B.R. Setting determination for numerical transformer differential protection via its detailed mathematical model. *IET Gener. Transm. Distrib.* **2020**, *14*, 1962–1972. [CrossRef]

7. Sevov, L.; Khan, U.; Zhang, Z. Enhancing Power Transformer Differential Protection to Improve Security and Dependability. *IEEE Trans. Ind. Appl.* **2017**, *53*, 2642–2649. [CrossRef]

8. Al-Ameri, S.M.; Kamarudin, M.S.; Yousof, M.F.M.; Salem, A.A.; Siada, A.A.; Mosaad, M.I. Interpretation of Frequency Response Analysis for Fault Detection in Power Transformers. *Appl. Sci.* **2021**, *11*, 2923. [CrossRef]

9. Al-Ameri, S.M.; Kamarudin, M.S.; Yousof, M.F.M.; Salem, A.A.; Banakhr, F.A.; Mosaad, M.I.; Abu-Siada, A. Understanding the Influence of Power Transformer Faults on the Frequency Response Signature Using Simulation Analysis and Statistical Indicators. *IEEE Access* **2021**, *9*, 70935–70947. [CrossRef]

10. Javed, U.; Mughees, N.; Jawad, M.; Azeem, O.; Abbas, G.; Ullah, N.; Chowdhury, M.S.; Techato, K.; Zaidi, K.S.; Tahir, U. A systematic Review of Key Challenges in Hybrid HVAC-HVDC Grids. *Energies* **2021**, *14*, 5451. [CrossRef]

11. So, E.; Verhoeven, R.; Simons, B.; Parks, H.V.; Angelo, D. A High-Precision Current Transformer for Loss Measurements of EHV Shunt Reactors. *IEEE Trans. Instrum. Meas.* **2019**, *68*, 1680–1687. [CrossRef]

12. Medeiros, R.P.; Costa, F.B. A Wavelet-Based Transformer Differential Protection with Differential Current Transformer Saturation and Cross-Country Fault Detection. *IEEE Trans. Power Deliv.* **2018**, *33*, 789–799. [CrossRef]

13. Ji, T.; Mo, C.; Zhang, L.L.; Wu, Q.H. Duty Cycle-Based Differential Protection Scheme for Power Transformers. *IEEE Trans. Power Deliv.* **2021**. [CrossRef]

14. Prodan, C.; Rata, G. Apparatus for determining the clock hour figure of the vector group of the electrical transformers. In Proceedings of the IEEE International Conference and Exposition on Electrical and Power Engineering (EPE), Iasi, Romania, 18–19 October 2018; pp. 0259–0263.

15. Zhang, Z.; Mo, M.; Wu, C. Three-phase distribution transformer connections modeling based on matrix operation method by phase-coordinates. *EURASIP J. Wirel. Commun. Netw.* **2021**, *2021*, 66. [CrossRef]

16. Saeed, H.; Kamel, M.; Karrar, A.; Eltom, A.H.; Bowman, M. On-Site Low Voltage Determination of Zero-Sequence Impedances for Power Transformers. *IEEE Trans. Power Deliv.* **2020**, *35*, 1048–1057. [CrossRef]

17. Xu, H.; Domínguez-García, A.D.; Sauer, P.W. Optimal Tap Setting of Voltage Regulation Transformers Using Batch Reinforcement Learning. *IEEE Trans. Power Syst.* **2020**, *35*, 1990–2001. [CrossRef]

18. Mitra, J.; Xu, X.; Benidris, M. Reduction of Three-Phase Transformer Inrush Currents Using Controlled Switching. *IEEE Trans. Ind. Appl.* **2020**, *56*, 890–897. [CrossRef]

19. Ge, W.; Zhao, J.; Wang, Y. Analysis of the residual flux influence on inrush current and electromagnetic force in large power transformer. *J. Eng.* **2019**, *2019*, 2426–2429. [CrossRef]

20. Gunda, S.K.; Dhanikonda, V.S.S.S.S. Discrimination of Transformer Inrush Currents and Internal Fault Currents Using Extended Kalman Filter Algorithm (EKF). *Energies* **2021**, *14*, 6020. [CrossRef]

21. Zheng, T.; Huang, T.; Ma, Y.; Zhang, Z.; Liu, L. Histogram-Based Method to Avoid Maloperation of Transformer Differential Protection Due to Current-Transformer Saturation under External Faults. *IEEE Trans. Power Deliv.* **2018**, *33*, 610–619. [CrossRef]
22. Shah, A.M.; Bhalja, B.R.; Patel, R.M.; Bhalja, H.; Agarwal, P.; Makwana, Y.M.; Malik, O.P. Quartile Based Differential Protection of Power Transformer. *IEEE Trans. Power Deliv.* **2020**, *35*, 2447–2458. [CrossRef]
23. Magrin, F.; Tavares, M.C. Increasing sensitivity for transformer protection using incremental differential. *J. Eng.* **2018**, *2018*, 1209–1215. [CrossRef]
24. GE Grid Solutions, P642: Transformer Protection IED, Technical Manual. Available online: https://www.gegridsolutions.com/app/viewfiles.aspx?prod=P64X&type=3 (accessed on 15 August 2021).
25. MiCOM S1 Agile Engineering Tool Suit (1.3.1), Alstom Grid. Available online: https://www.gegridsolutions.com/multilin/catalog/engineering-tool-suite.htm (accessed on 5 August 2021).
26. Ameli, A.; Ghafouri, M.; Zeineldin, H.H.; Salama, M.M.A.; El-Saadany, E.F. Accurate Fault Diagnosis in Transformers Using an Auxiliary Current-Compensation-Based Framework for Differential Relays. *IEEE Trans. Instrum. Meas.* **2021**, *70*, 1–14.
27. IEEE Draft Standard for Common Format for Transient Data Exchange (COMTRADE) for Power Systems. In *IEEE PC37.111/D4, January 2012 (IEC 60255-24 Ed.2)*; IEEE: Manhattan, MY, USA, 2012; pp. 1–72.
28. SEL-5030 SynchroWAVE Acselerator QuickSet Software, Schweitzer Engineering Laboratories, Inc. Available online: https://selinc.com/products/5030/ (accessed on 10 August 2021).